NASA-49 (05)

Semiclassical Theory of Elastic Perturbation *

R. P. Marchi
Stanford Research Institute
Menlo Park, California 94025

The Stueckelberg formulation for transition probabilities is utilized to explain perturbation effects observed in elastic differential cross section measurements. The model based on a competing trajectory concept implies oscillating cross sections for all inelastic processes occurring by means of a curve crossing mechanism. Variations are made in the slopes of two crossing potential energy curves to determine the effect on the cross section. The model gives qualitative agreement with experiment, but definitive tests must await more accurate potential energy curves.

* Supported by National Aeronautics and Space Administration and Stanford Research Institute

INTRODUCTION

Several years ago excellent experimental differential cross section measurements of ion-atom scattering processes[1] began appearing which under continuing investigation have yielded a wealth of information.[2,3] Among the features that have been noted is a small oscillatory behavior called an "elastic perturbation" whose origin has been attributed to the crossing of two molecular electronic energy curves.[2] This perturbation has been observed in four different systems: He^+ - Ne, He^+ - Ar, Ar^+ - Ar, He^+ - He ($^4He^+$ - ^4He, $^4He^+$ - ^3He, $^3He^+$ - ^3He). Effects of similar appearance have been observed in several other systems,[4] but the experimental conditions in these cases have made it extremely difficult to isolate the origin of these anomalies. The abundance of curve crossings in most atomic and molecular systems would indicate that the elastic perturbation should be seen at some angular range in most differential cross section measurements.

As its name implies, the elastic perturbation is a small feature and thus has only slight effects on quantities such as total cross sections. When its origins are understood, however, its implications overshadow its minor perturbing effect: it not only permits the location and characterization of curve crossings, but it also acts as a bridge between elastic and inelastic scattering theory, since even though it is basically an elastic process, more than one energy state is involved. Furthermore, it clearly implies an oscillatory behavior for inelastic differential cross sections.

Figure 1 shows typical differential cross sections for several systems in which the elastic perturbation has been observed. The perturbation appears very clearly in the He^+ - Ar data and to a lesser extent in the He^+ - Ne data as an undulation superimposed on a monotonically decreasing cross section. The oscillations cover a wide range of angles, and whether this is due to one curve crossing or several is difficult to determine. Because He^+ - He

is a symmetric system, its data is complicated by the presence of major oscillations arising from the interference between the gerade and ungerade energy curves.[5] The perturbation can be perceived, however, in the vicinity of 18^0 where a peak is abnormally high and the surrounding peaks and valleys are distorted. Data of this nature has also been published for the Ar^+ - Ar system,[1] for which perturbations can be observed at $E\theta \simeq 2200$ eV deg., but in this case the data is complicated by the large number of possible competing states and it is difficult to make an unambiguous analysis.

The connection between elastic perturbations and curve crossings was made by means of a knowledge of the appropriate potential energy curves and semiclassical arguments relating location of the anomaly in scattering angle to distance of closest approach and thus to a region of the potential. For He_2^+ the crossing was estimated to be at 0.90 A, while a priori calculations[6] indicated the crossing (or pseudocrossing) of two $^2\Sigma_g$ states at 0.80 A. For the He^+ - Ne system the crossing was estimated to be at 1 A, and calculations by Michels[7] indicate a crossing at 0.93 A between a $^2\Sigma$ and a $^2\Pi$ state. The $^2\Pi$ state arises from a ground state He atom and a ground state Ne^+. This type of crossing was recently discussed by Lichten.[8]

To date the most systematic experimental study of the elastic perturbation has been performed on the He^+ - He system.[9] Before the perturbation for this system can be characterized, extensive numerical analysis of the data will be needed to separate the interference pattern of the gerade and ungerade states from the pattern of the elastic perturbation. On the other hand, the He_2^+ molecule has only three electrons, and so accurate a priori calculations of the appropriate potential energy curves are available.

In this paper it will be assumed that the elastic perturbation arises from the crossing of only two electronic states and that the energies are small enough that any effects due to the momentum of the electrons and Coriolis forces can be ignored. Our object will will to determine whether such a simple theory is sufficient to produce general agreement with experiment and to provide some insight into the details of curve crossing phenomena.

THEORY

The two-state problem, whether it be an elastic or inelastic process, is governed by a pair of coupled equations:

$$\frac{d^2\chi_1(r)}{dr^2} + \left[k_1^2 - U_{11}(r) - \frac{\ell(\ell+1)}{r^2}\right] \chi_1(r) = U_{12}(r)\chi_2(r) ,$$

$$\frac{d^2\chi_2(r)}{dr^2} + \left[k_2^2 - U_{22}(r) - \frac{\ell(\ell+1)}{r^2}\right] \chi_2(r) = U_{21}(r)\chi_1(r) , \quad (1)$$

where U_{ii} are the potentials for the respective states and U_{ij} is the interaction energy between the initial and final states. The origin and general properties of these equations have been extensively discussed elsewhere.[10] While the general behavior of Eqs. (1) is known, their numerical solution is beset with convergence problems and, as yet, very few results have been obtained for this type of scattering problem. The approach here is a much simpler one and necessarily is only approximate. Its formulation ensures at least qualitative agreement with experiment and thus, although the treatment is not rigorous, it is informative.

The model used in this paper is most easily understood by examining hypothetical potential energy curves for two states A and B involved in a collisions (see Figure 2). These potentials are not adiabatic states but rather are diabatic energy levels that might be expected when the internuclear velocity is nonzero.[8] Thus, there is no avoided crossing, but instead the potentials are allowed to cross. The adiabatic curves are indicated by the dashed lines. An elastic collision between A and B corresponds to entering and exiting along pathway 1. At small internuclear distances the collision may proceed along pathway 2 or 3, and, in fact, depending upon the radial velocity, it may follow both. For values of the radial velocity approaching zero the collision proceeds exclusively along the adiabatic curve, that is, pathways 1 and 3. For large velocities it will proceed along the diabatic pathway, curves 1 and 2. For

intermediate velocities pathways 2 and 3 compete, giving rise to an interference pattern. It is this interference that is responsible for the elastic perturbation.

Inelastic processes can be considered as complementary to the elastic perturbations; the only difference is an exit along pathway 4 rather than 1. Inelastic differential cross sections therefore should always exhibit undulatory behavior. Likewise, if additional curve crossings are involved, perturbations may also appear in the inelastic measurements.

The primary problem in performing quantitative calculations of the elastic perturbation, or of an inelastic process for that matter, is the determination of the probability that the collision follows a particular path. These probabilities can be obtained either from the solution of Eqs. (1) or by means of approximations.

The most widely discussed approximation is the Landau-Zener formula. Derived independently by Landau, Zener, and Stueckelberg, it has been used many times in the calculation of total cross sections. Derivations and essential assumptions are given in many text books[10] and will not be repeated here. Its validity and limitations have been discussed by numerous authors,[11] and possible improvements have been suggested by Coulson and Zalewski.[12] The Landau-Zener formula relates the probability, p, of crossing from one adiabatic curve to another (i.e., of remaining on a single diabatic curve) to several parameters describing the physical characteristics of the crossing:

$$
\begin{aligned}
p(E,\ell) &= \exp(-v_0/v_r(E,\ell)) \quad , \\
v_0 &= H_{12}(R_x)/\hbar\left|V_1' - V_2'\right|_{R_x} \quad , \\
vr^2(E,\ell) &= \frac{2}{\mu}\left[E - V_1(R_x) - \frac{\hbar^2(\ell+\frac{1}{2})^2}{2\mu R_x^2}\right]
\end{aligned}
\tag{2}
$$

where v_0 is a characteristic velocity defined by the shape of the crossing. H_{12} is the perturbation Hamiltonian between the two states;

at the crossing point its value is equal to 1/2 the difference between the adiabatic energies. V_i' is the slope of one of the diabatic potentials evaluated at the crossing point. v_r is the radial velocity and is dependent upon the incident energy and the angular momentum. Since the Landau-Zener formula assumes that the transition occurs only at the crossing point, all quantities are evaluated at R_x. For values of ℓ such that v_r is imaginery, p is taken equal to unity.

For the elastic perturbation the necessary probabilities are easily ascertained from Fig. 2. One possible trajectory is along pathway 1 to 2 and back out along 1; that is, the diabatic curve is followed throughout the collision. This involves two transitions, so the probability is

$$P_d(\ell) = p^2(\ell) \quad . \tag{3}$$

The other possibility is to follow the adiabatic route: $1 \rightarrow 3 \rightarrow 1$. The corresponding probability is

$$P_a(\ell) = [1 - p(\ell)]^2 \quad . \tag{4}$$

These probabilities modulate the interference between the two possible trajectories the differential cross section is thus written

$$d\sigma(\theta) = \left| f^d(\theta) + f^a(\theta) \right|^2 \quad , \tag{5}$$

$$f^j(\theta) = \frac{1}{2ik} \sum_{\ell} (2\ell+1)[P_j^{1/2}(\ell) e^{2i\delta_j(\ell)} - 1] P_\ell(\cos\theta) \quad . \tag{6}$$

If the semiclassical approximations of Ford and Wheeler [13] are now applied, the cross section becomes

$$d\sigma(\theta) = \left| P_d \bar{\sigma}_d^{1/2} e^{iA_d/\hbar} + P_a \bar{\sigma}_a^{1/2} e^{iA_a/\hbar} \right|^2 \tag{7}$$

Here $\bar{\sigma}_j$ is the classical expression for the differential cross section:

$$\sigma_j = b_j / (\sin\theta \left| d\theta/db_j \right|) \quad , \tag{8}$$

where b_j is the impact parameter for the appropriate adiabatic or diabatic potential, and it is related to the angular momentum

quantum number, ℓ, by the relation $(\ell + \frac{1}{2}) = bk$. The A_j can be taken as the classical actions and are readily calculated from the phase shift and deflection function:[14]

$$A_j = 2\hbar\delta_j - (\ell + \tfrac{1}{2})\hbar\theta \quad . \tag{9}$$

Eqs. (7) and (9) become much more complicated when rainbow scattering is involved.

It is clear that this model, cast in the form of Eq. 8, is the one put forth by Stueckelberg some 30 years ago. Recently Green and Johnson[15] investigated this and similar approaches to curve crossing phenomena and applied the results to electron capture processes for H^+ - He and other asymmetric systems.

If this model is applied to a symmetric system, such as He_2^+, additional energy paths must be considered because of the ungerade-gerade symmetry. In He_2^+ the lowest lying ungerade curve has no crossing and for exploratory purposes it will be assumed that gerade curve has only one crossing of interest. The cross section is given by

$$d\sigma = \tfrac{1}{4}\left| f_u + f_g^d + f_g^a \right|^2 \quad , \tag{10}$$

where u and g refer to the ungerade or gerade potential and a and d refer to the adiabatic or diabatic energy paths discussed in the previous paragraphs. Since the ungerade potential has no crossings,

$$f_u = \frac{1}{2ik}\Sigma(2\ell+1)\,(e^{2i\delta_\ell} - 1)\,P_\ell(\cos\theta) \quad . \tag{11}$$

In the above expressions nuclear symmetry effects arising from the participation of identical atoms in the scattering process are ignored; these effects have been discussed elsewhere,[3,5] and their inclusion here would only serve to cloud the issue. In this study phase shifts were evaluated by the WKB approximation. The use of this approximation is valid at these energies,[16] and the integrals are evaluated by Gauss-Mehler quadratures.[17] For the cases shown here the cross sections were evaluated by means of Eqs. (5) and (6).

In general about 1600 partial waves were required to obtain convergence within one percent. In a few cases the cross sections were also evaluated by means of Eq. (7). For angles somewhat larger than the threshold angle the methods gave identical results. The advantage of the Ford and Wheeler semiclassical procedure lies not in the ease of calculations (even that is lost in the rainbow region), but rather the tremendous physical insight that it brings to the problem. The capability of relating scattering angles to specific impact parameters in regions of the potential is a powerful tool.

RESULTS

A difficult problem exists in applying this type of model to actual systems because the selection of a diabatic curve is arbitrary. The main reason for this difficulty is that, unlike adiabatic states, working definitions of diabatic states have not come into acceptance. O'Malley [18] has recently proposed a prescription for the determination of diabatic states, but it has not as yet been applied. In order to circumvent this problem, empirical diabatic states can be constructed from adiabatic potential energy curves. The difficulty here is that the adiabatic ab initio calculations are usually performed at intervals of internuclear separation that are too wide to permit any unambigious determination of the shape of the curves in the crossing region. For this reason the calculations reported in this paper were performed on a number of potentials in order to test the sensitivity of the differential cross section to the shape of the potentials in the crossing region.

The potentials are shown in Fig. 3a. Curve 1 is a simple monotonic repulsive potential which could be considered as a typical diabatic energy curve. Curve 2 corresponds to an adiabatic potential. Actually it is the ground state $^2\Sigma_g^+$ of the He_2^+ system. Curve 3 is characterized by a discontinuous change in the first derivative of the potential at the crossing point. Curve 4 maintains a smooth change in the first derivative of the potential. Figure 3b displays the deflection function Θ, versus distance of closest approach r_0, for the

corresponding potentials showns in Fig. 3a. The shape of these curves is most easily understood by examining the expression for the deflection function written in the following way:[14]

$$\Theta = -\frac{b}{E}\int_{r_0}^{\infty} \frac{r(dV/dr)}{\left(1-\frac{V}{E}\right)\left(1-\frac{V}{E}-\frac{b^2}{r^2}\right)^{\frac{1}{2}}}\,\frac{dr}{r^2} \quad . \tag{12}$$

The main contribution to this integral comes from the region of r_0 the classical distance of closest approach. A heuristic justification of this fact is that the radial motion of the nuclei is slowest in the region of r_0, and thus the time available for a perturbing force to act is longest. Thus, if dV/dr has a sudden change, say a decrease, in the region $r \approx r_0$, then Θ will exhibit a sudden change, in this case a decrease. Even a region of constant potential ($dV/dr = 0$) will cause a minimum in the deflection function, as is shown by curve 2 of Figs. 3a and 3b.

Typical cross sections resulting from these potentials are shown in Figs. 4 through 6 for various values of the Landau-Zener parameter, v_0. For comparison in these cases $v_\infty = 6.9 \times 10^6$ cm/sec. In each figure the dashed line represents the cross section arising from a single potential — the diabatic curve 1 in Fig. 2. Changing v_0 does not change the frequency of the interference pattern, but only the amplitudes, as can easily be seen by inspection of Eq. (7). As the scattering angle increases the radial velocity, $\bar{v}_r(R_x)$, increases, and so the contribution from the adiabatic curve decreases so that the cross section becomes extremely damped, oscillating about the cross section from the diabatic curve. Inspection of Eq. (7) shows that the frequency of the oscillations is governed by the difference in the classical actions which in turn are roughly proportional to the spacing between the two potential curves. The greater this difference, the more frequent are the oscillations. Thus Fig. 6 exhibits more oscillation than Fig. 5, and the frequency of oscillations in Fig. 5 is greater than that in Fig. 4. Although all the figures shown are for one incident energy (50 eV, center-of-mass), results at other energies are very similar and not unexpected.

The behavior of an interference pattern with respect to the energy has been discussed elsewhere[14] and has been shown to vary, to a first approximation, as the square root of the energy. That is, increasing the energy by a factor of 4 approximately doubles the frequency of oscillations with respect to θ. The variation of the amplitudes with energy is more complicated and depends upon the behavior of Eqs. (2) and (8).

The surprising feature of these cross sections is the location of the onset of the interference pattern. Using a classical interpretation, the threshold value for the scattering angle, θ_x, is determined by examination of the deflection function as in Fig. 3b. For the case involving curve 2, a value of $\theta_x^2 = 27^0$ would be expected and similarly $\theta_x^3 = 34^0$ and $\theta_x^4 = 38^0$. Inspection of Figs. 4 through 6 clearly shows in each case, however, that θ_x is less than these expected values. For the cases involving potential curves 2 and 3 the situation is complicated, since the corresponding deflection functions each possess a minimum. A minimum in the deflection function gives rise to a phenomenon called rainbow scattering,[13] an effect which not only creates additional oscillations, but also shifts the appearance of the undulations to smaller angles. However, the case corresponding to potential curve 4 is not encumbered by these additional complications and can be more readily analyzed. Here, classically, the threshold angle would be expected at 38^0, while it actually appears around 32^0. This discrepancy points out the different results produced by a partial wave calculation [Eq. (6)] and by a semiclassical approximation [Eq. (7)]. Because of the use of the stationary phase approximation, the semiclassical approximation permits only one partial wave to contribute to the cross section at a given angle and also establishes a unique relation between the scattering angle and the impact parameter. Because the probability function, p, as a function of the impact parameter posesses a discontinuity, the semiclassical approximation gives a sudden onset to the interference pattern at that angle corresponding to the impact parameter where the probability abruptly changes from 1 to 0.

The partial wave treatment, on the other hand, constructs the cross section from the contribution of many partial waves. The major contribution comes from those partial waves that immediately surround the wave corresponding to the semiclassical stationary phase. As a result the partial wave expansion does not possess the sharp features introduced by the semiclassical approximation, and the onset of the interference pattern appears at an angle smaller than the semiclassical θ_x. For angles somewhat larger than θ_x the two procedures give identical results. Also, as the energy is increased, the agreement between two methods increases in the threshold region.

This discrepancy between the partial wave and semiclassical calculations is important, since attempts to use the elastic perturbation phenomena to locate curve crossings have utilized a classical type of analysis. In the two cases where it has been applied, He^+ - He, and He^+ - Ne, the interpretation of the experimental data yielded values for the crossing location that were larger than ab initio theoretical calculations indicated. This is as it should be, for the classical analysis of the data can only yield an upper limit to the location of the curve crossing.

Figure 7 shows the differential cross sections resulting from three states, two of which cross. This situation corresponds to that of Eq. (9) and resembles closely the case of He^+ scattering from He. The gerade potentials[5] used in the calculation of Fig. 7 are curves 1 and 4 of Fig. 3a; the ungerade potential is the lowest lying $^2\Sigma_u^+$ state of He_2^+, and it is taken from the work of Gupta and Matsen[6] suitably extended by means of screened coulomb and r^{-4} functions.

CONCLUSION

Figures 4 through 7 indicate that the model here described does produce general agreement with present experimental results. The agreement could certainly be improved, but the improvement would be of questionable value. At this time there are simply too

many parameters to obtain agreement with the onset of the elastic perturbation, and the frequency and the amplitude of the oscillations. Furthermore, there is the question of an additional phase shift due to the crossing alone. Thorson[11] states that for rapid passage and weak coupling an additional shift of $\pi/4$ is introduced, while Mott and Massey[10] obtain $\pi/2$. In any case inclusion of this additional shift does not qualitatively change the results. It emphatically emphasizes the need for a rigorous treatment of the problem.

There is one feature, however, that differs significantly from the observations. Experimentally the perturbation appears to extend over a limited range of the scattering angle. This model produces results covering a much larger range in angle. On the one hand, this discrepancy could be due to the failure of the Landau-Zener probability to decay rapidly enough with an increase in the radial velocity at the crossing point. This is equivalent to saying that as the scattering angle increases the probability remains too large. On the other hand, it must be realized that perhaps the experimental oscillations fade out for different reasons. In most real systems isolated curve crossings are rare, although ion-ion recombination problems are a notable exception. With many crossings participating in the scattering process it could well be that the oscillations are simply washed out by the competing contributions from many scattering amplitudes.

In conclusion further understanding of collision phenomena requires elucidation of the concept of diabatic states and rigorous treatment of the multistate problem. Quantal solutions are especially needed near the threshold in angle and energy in order to complement semiclassical methods which presumably will be validated in the region away from the crossing.

ACKNOWLEDGMENT

The author wishes to express his appreciation to Dr. F. T. Smith for helpful discussions.

REFERENCES

1. D. C. Lorents and W. Aberth, Phys. Rev. 139, A1017 (1965). W. Aberth and D. C. Lorents, Phys. Rev. 144, 109 (1966).

2. F. T. Smith, D. C. Lorents, W. Aberth, and R. P. Marchi, Phys. Rev. Letters, 15, 742 (1965).

3. W. Aberth, D. C. Lorents, R. P. Marchi and F. T. Smith, Phys. Rev. Letters, 14, 776 (1965). F. T. Smith, R. P. Marchi, W. Aberth, D. C. Lorents, and O. Heinz, Phys. Rev. 161, 31 (1967).

4. V. V. Afrosimov, Yu. S. Gordeev, A. M. Polyansky, and A. P. Shergin, V International Conference on the Physics of Electronic and Atomic Collisions, Leningrad, 1967 (Publishing House "Nauka," Leningrad, USSR, 1967), p. 475. H. H. Fleischmann and R. A. Young, ibid., p. 472.

5. F. J. Smith, Proc. Phys. Soc. (London) 84, 889 (1964). R. P. Marchi and F. T. Smith, Phys. Rev. 139, A1025 (1965).

6. B. K. Gupta and F. A. Matsen, J. Chem. Phys. 47, 4860 (1967).

7. H. H. Michels, private communication.

8. W. Lichten, Phys. Rev. 164, 131 (1967).

9. W. Aberth and D. C. Lorents, unpublished results.

10. N. F. Mott and H.S.W. Massey, The Theory of Atomic Collisions (Oxford at the Clarendon Press, Great Britain, 1965), 3rd ed.

11. O. K. Rice, J. Chem. Phys. 3, 386 (1935). D. R. Bates, Proc. Roy. Soc. (London) A257, 22 (1960). W. R. Thorson and S. A. Boorstein, IV International Conference on the Physics of Electronic and Atomic Collisions, (Science Bookcrafters, Inc., Hastings on Hudson, New York, 1965), p. 218. J. V. Greenman, Phys. Rev. 163, 119 (1967).

12. C. A. Coulson and Z. Zalewski, Proc. Roy. Soc. (London) 268, 437 (1962).

13. K. W. Ford and J. A. Wheeler, Ann. Phys. 7, 259 (1959).

14. F. T. Smith, R. P. Marchi, and K. G. Dedrick, Phys. Rev. 150 79 (1966).

15. T. A. Green and R. E. Johnson, Phys. Rev. 152, 9 (1966).

16. R. J. Munn, E. A. Mason, and F. J. Smith, Institute of Molecular Physics, University of Maryland. IMP-NASA-38, 1964.

17. F. J. Smith, Physica 30, 497 (1964).

18. T. F. O'Malley, V International Conference on the Physics of Electronic and Atomic Collisions, Leningrad, 1967 (Publishing House "Nauka," Leningrad, USSR, 1967), p. 348.

FIGURE CAPTIONS

Fig. 1. Examples of elastic perturbation effects observed in differential elastic scattering patterns. Figure is taken from ref. 2. The data was originally published in ref. 1.

Fig. 2. Schematic representation of diabatic potential energy curves for a diatomic system A-B. Adiabatic curves are shown by the dashed lines.

Fig. 3a. Potential energy curves used in the calculations in this paper. Curves 1 and 2 actually correspond to the $^2\Sigma_g^+$ states of He_2^+ and are taken from ref. 6 and 7. For small values of r these curves were extended by means of a screened coulomb function and at large distances by an r^{-4} function.

Fig. 3b. Classical deflection function versus classical distance of closest approach, r_0, for the corresponding potentials shown in Fig. 3a. The impact parameter is related to r_0 by $b = r_0(1-V(r_0)/E)$.

Fig. 4. Differential cross sections versus scattering angle for potentials 1 and 4 shown in Fig. 3a. All quantities are in the center of mass coorindate system. --- is for potential 1 alone; —— is for potentials 1 and 4 with $v_0 = 4.65 \times 10^6$ cm/sec (Eq. 2); —·—— is for potentials 1 and 4 with $v_0 = 3.80 \times 10^7$ cm/sec.

Fig. 5. Differential cross section versus scattering angle for potentials 1 and 3 with $v_0 = 2.03 \times 10^6$ cm/sec.

Fig. 6. Differential cross section versus scattering angle for potentials 1 and 2 with $v_0 = 9.50 \times 10^6$ cm/sec.

Fig. 7. Differential cross section versus scattering angle calculated by means of Eq. (10). Here $v_0 = 8.54 \times 10^5$ cm/sec and the appropriate potentials are discussed in the text.

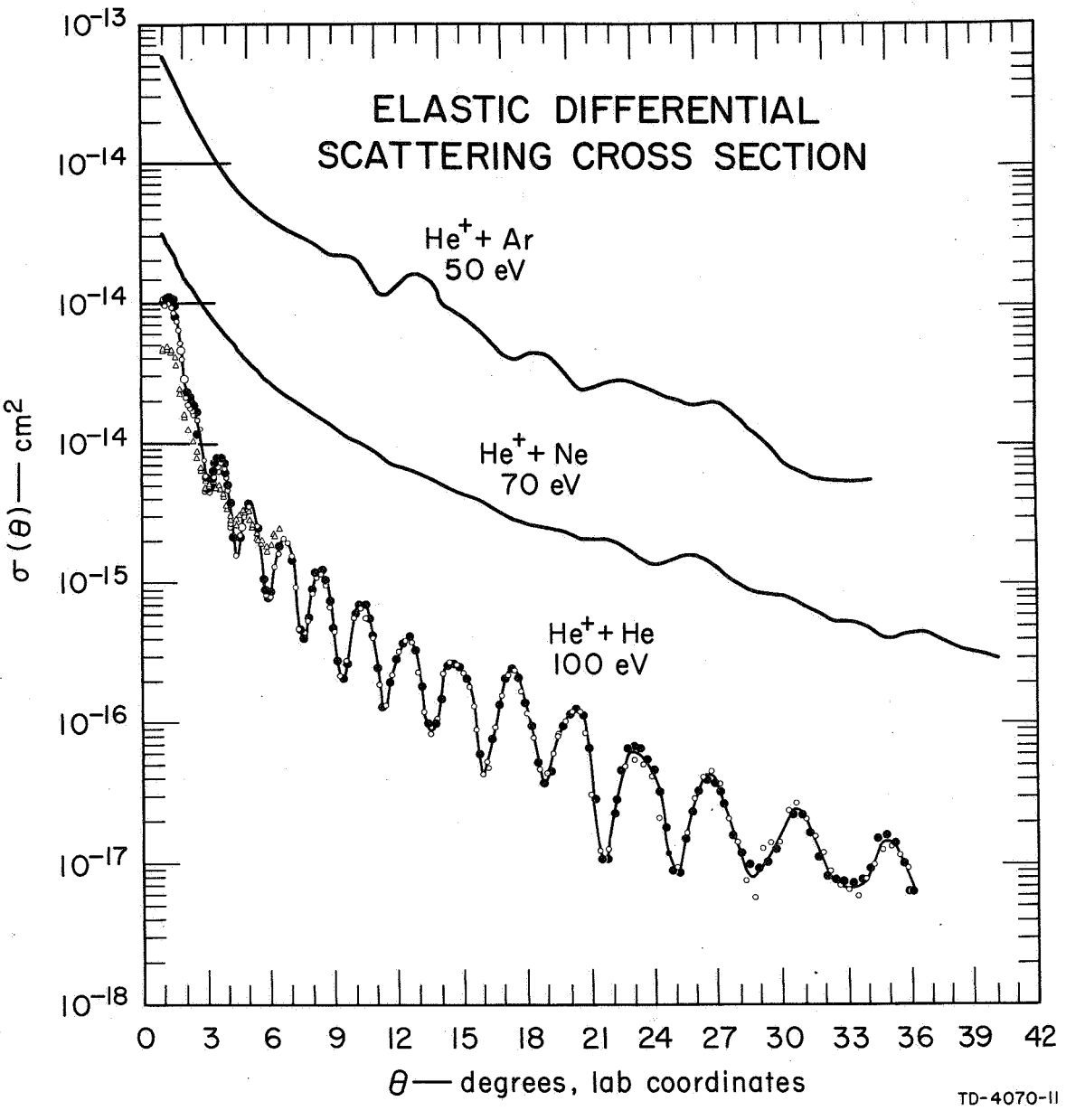
ELASTIC DIFFERENTIAL
SCATTERING CROSS SECTION
He+ + Ar
50 eV
He+ + Ne
70 eV
He+ + He
100 eV
σ (θ) — cm2
θ — degrees, lab coordinates
TD-4070-11

FIG. 1

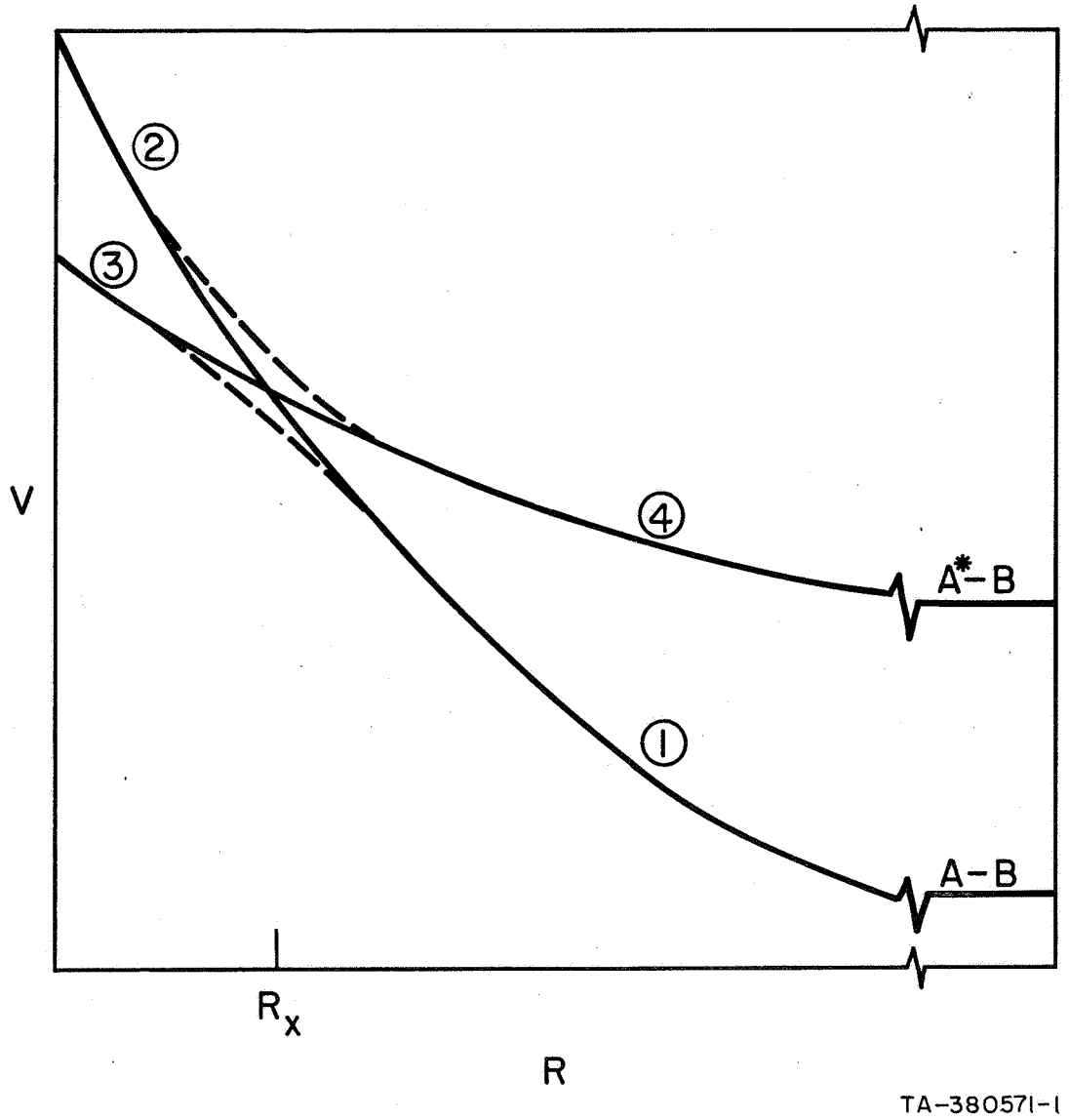

FIG. 2

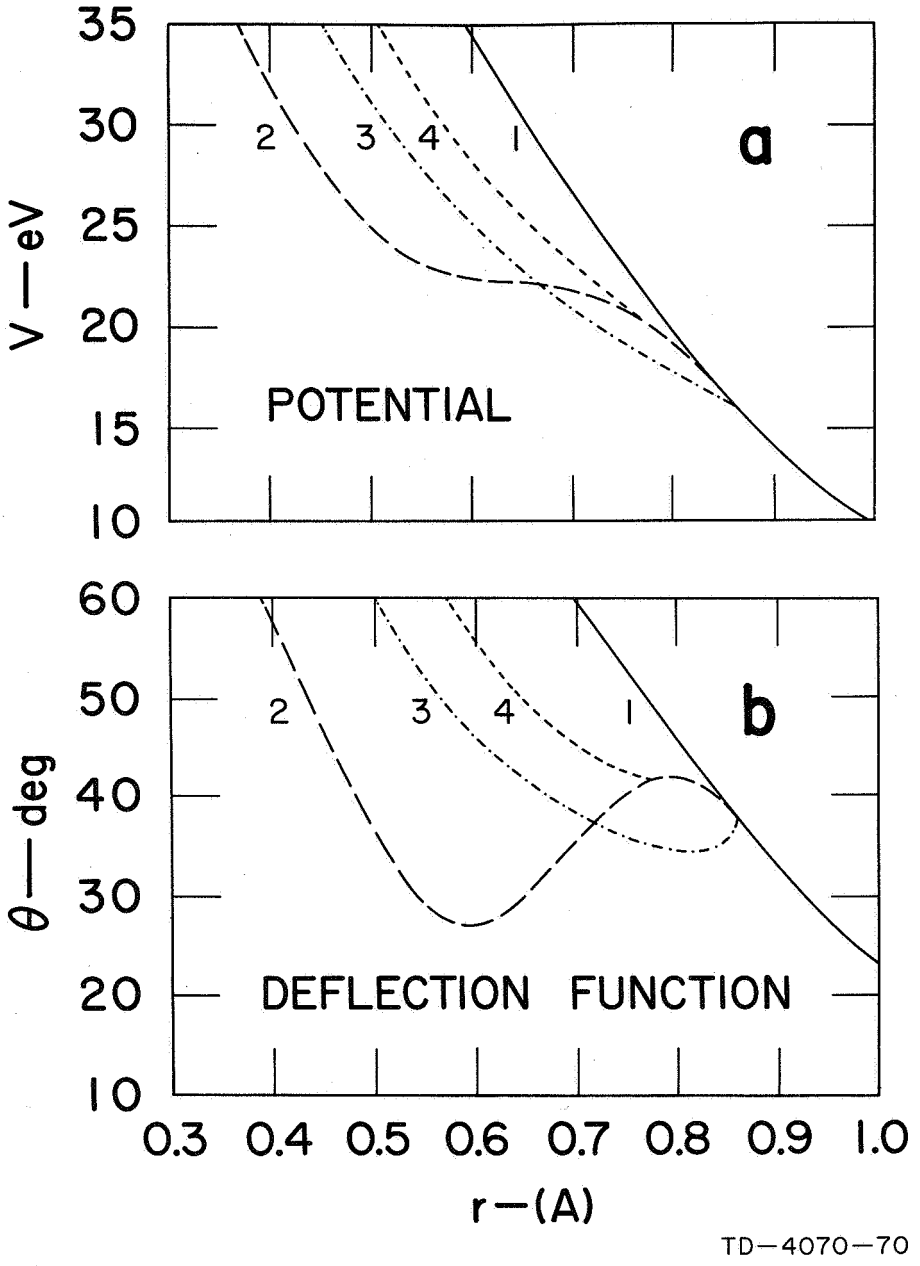
35
30
25
20
15
10
V — eV
2
3
4
1
a
POTENTIAL
60
50
40
30
20
10
θ — deg
2
3
4
1
b
DEFLECTION FUNCTION
0.3
0.4
0.5
0.6
0.7
0.8
0.9
1.0
r — (A)
TD—4070—70

FIG. 3

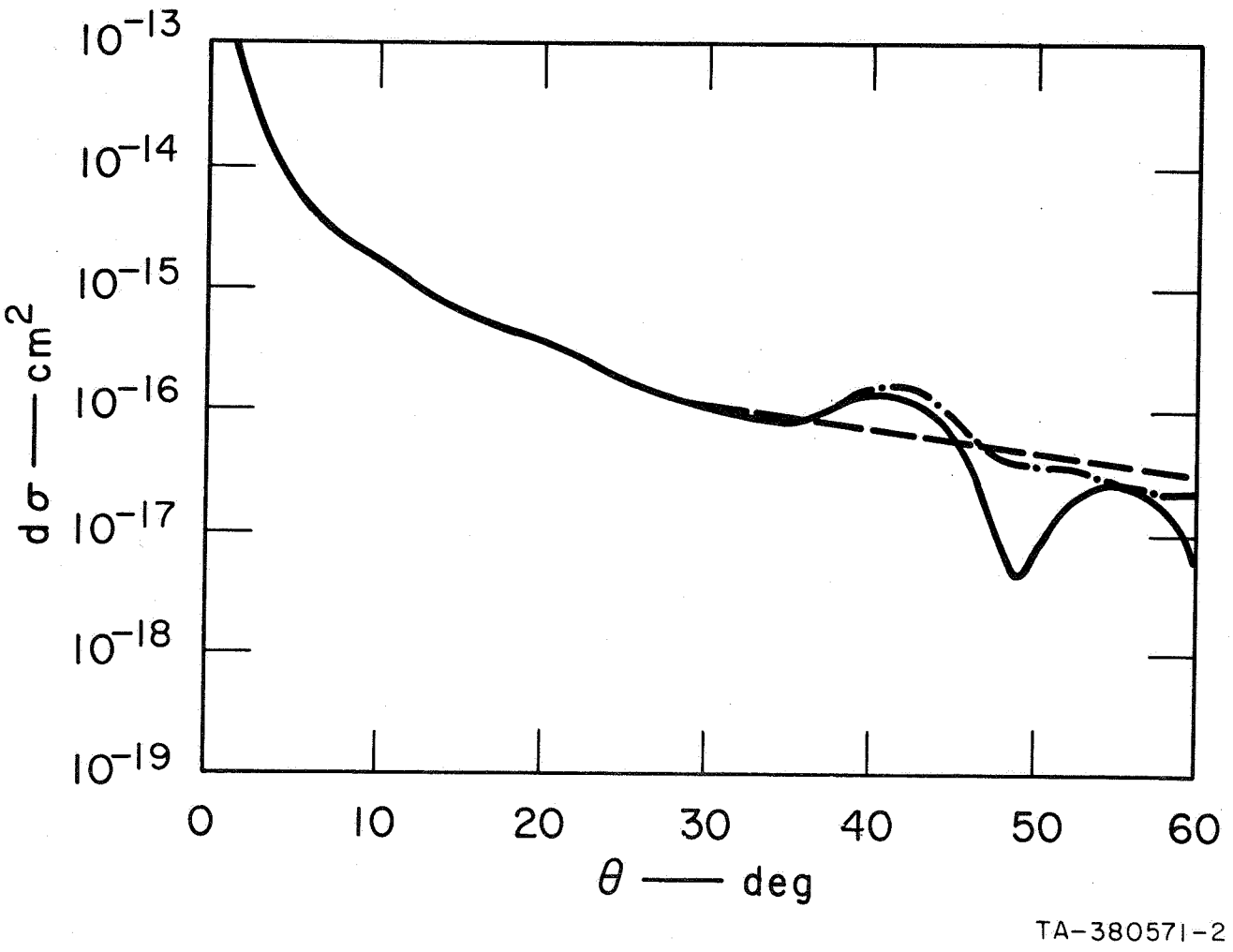
10^{-13}
10^{-14}
10^{-15}
10^{-16}
10^{-17}
10^{-18}
10^{-19}
$d\sigma$ — cm^2
0
10
20
30
40
50
60
θ — deg
TA-380571-2

FIG. 4

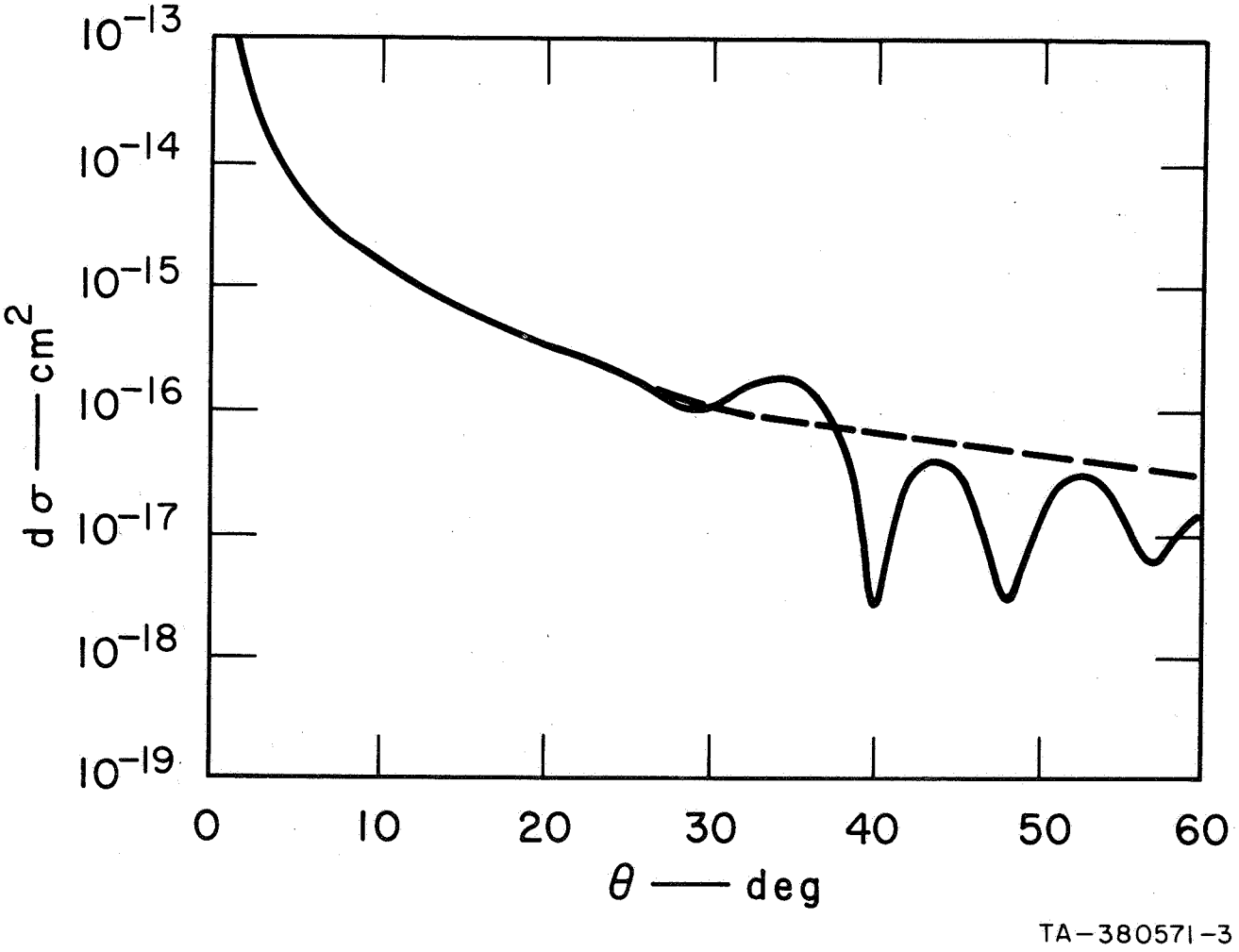
10^{-13}
10^{-14}
10^{-15}
10^{-16}
10^{-17}
10^{-18}
10^{-19}
$d\sigma$ — cm^2
0
10
20
30
40
50
60
θ — deg
TA-380571-3

FIG. 5

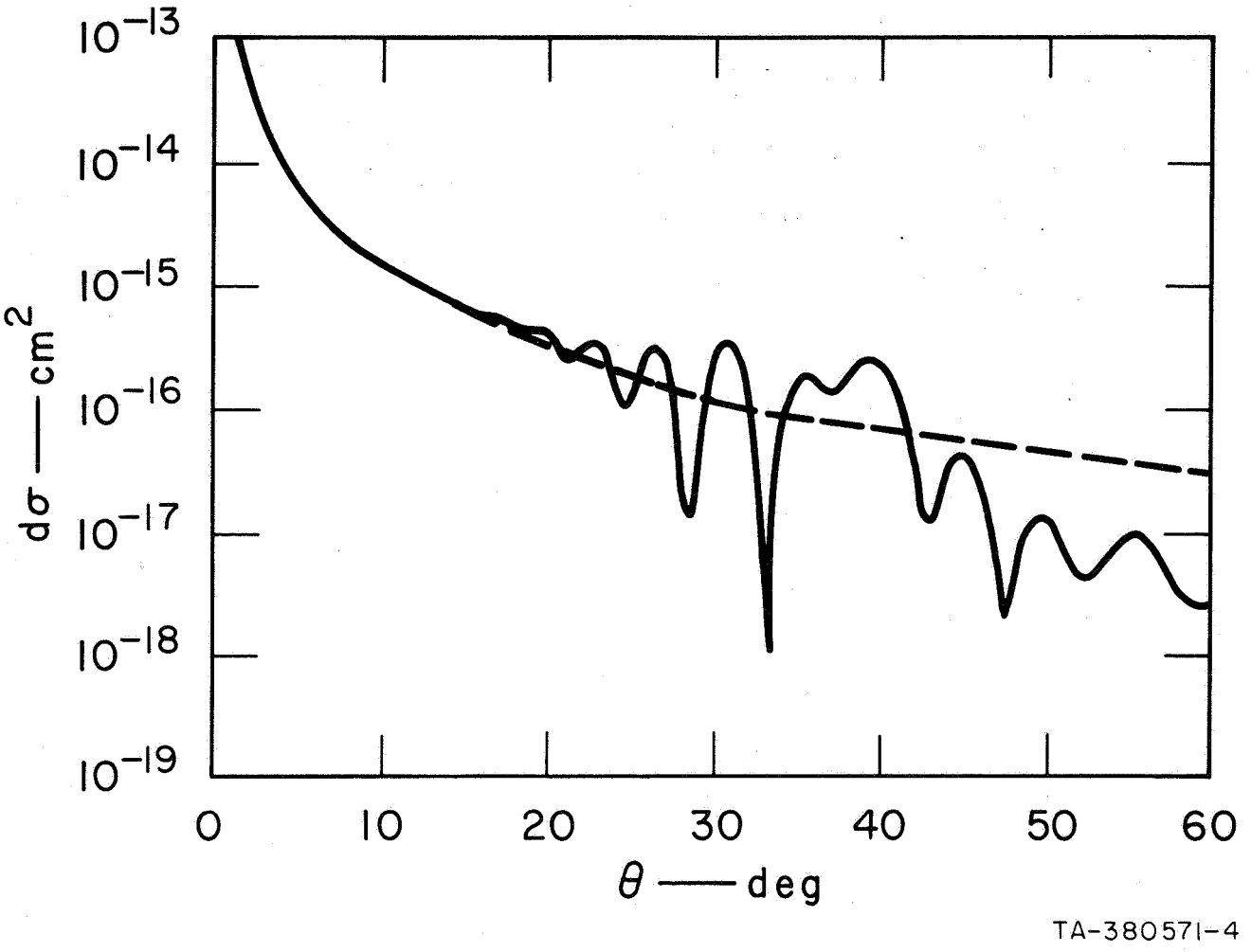
10^{-13}
10^{-14}
10^{-15}
10^{-16}
10^{-17}
10^{-18}
10^{-19}
$d\sigma$ — cm^2
0
10
20
30
40
50
60
θ — deg
TA-380571-4

FIG. 6

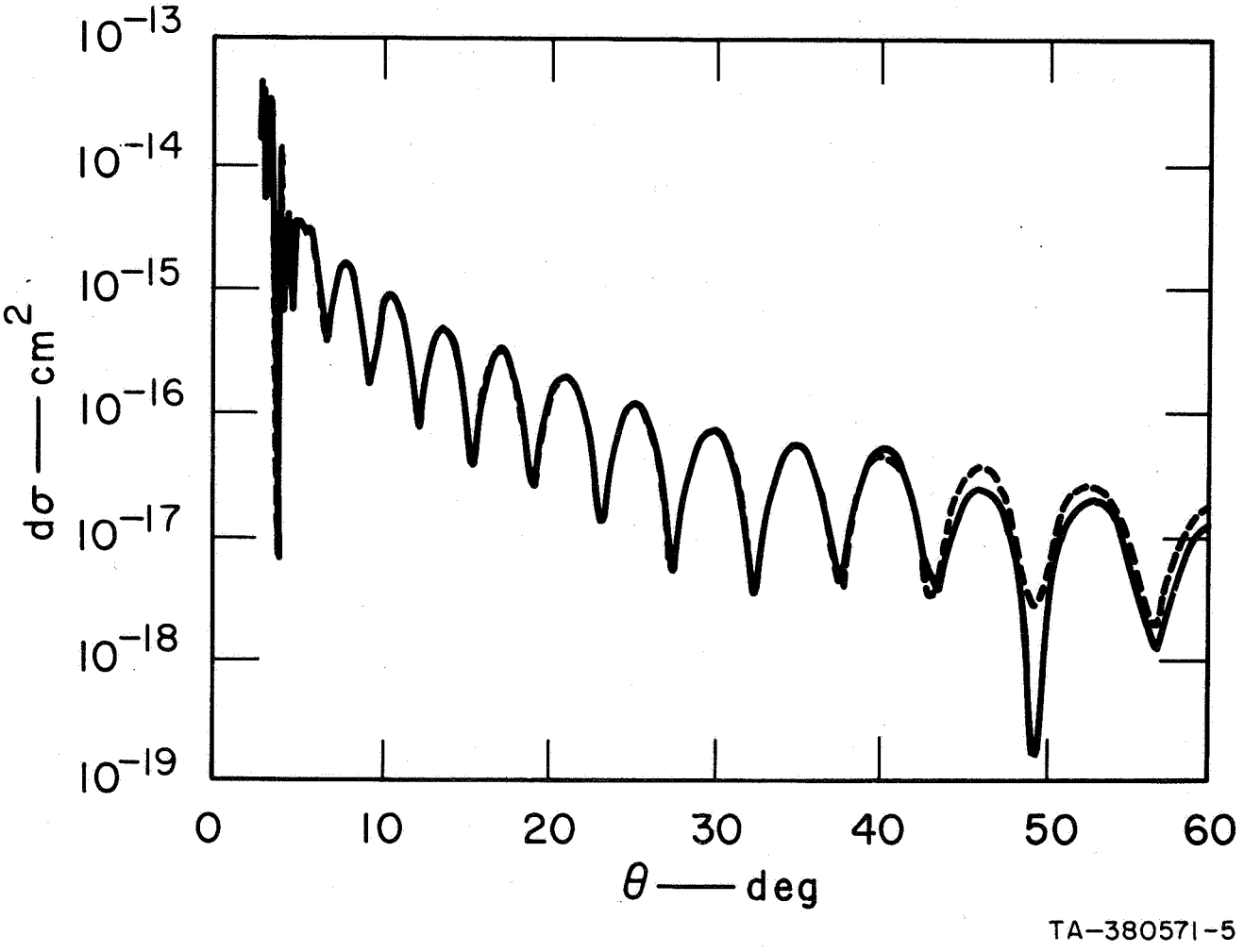
10^{-13}
10^{-14}
10^{-15}
10^{-16}
10^{-17}
10^{-18}
10^{-19}
$d\sigma$ — cm^2
0
10
20
30
40
50
60
θ — deg
TA-380571-5

FIG. 7